iScience

CellPress
OPEN ACCESS

Article

SENP1 facilitates OM-MSC differentiation through activating OPTN-mediated mitophagy to mitigate the neurologic impairment following ICH

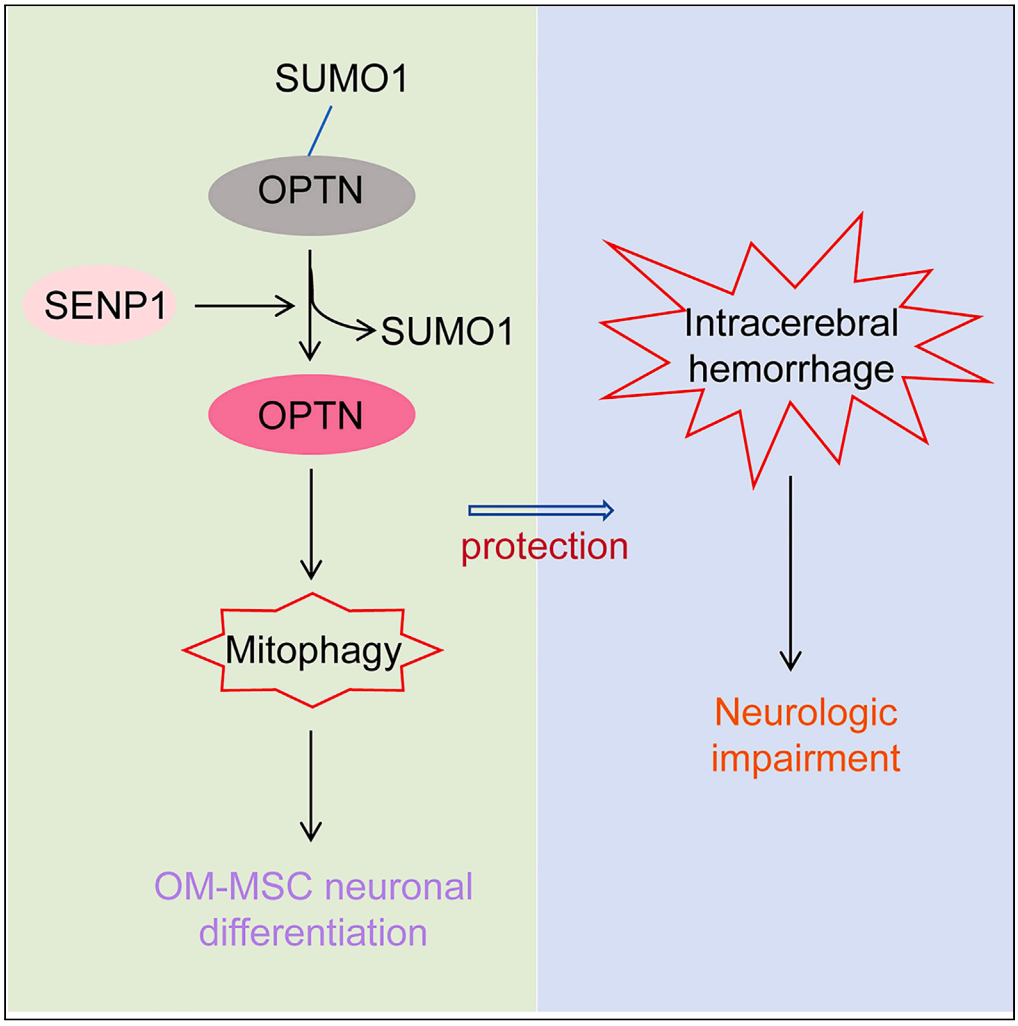

Jun He, Jun Peng, You Li, ..., Long Lin, Jian Wang, Ying Xia

xiaying0509@163.com

Highlights

SENP1 promotes the neuronal differentiation of OM-MSCs

SENP1 reduces post-ICH neuron damage by regulating OM-MSC neuronal differentiation

SENP1 regulates mitophagy via regulating the SUMOylation of OPTN

OPTN promotes OM-MSC neuronal differentiation to alleviate ICH-caused neuron damage

He et al., iScience 27, 109865
June 21, 2024
https://doi.org/10.1016/j.isci.2024.109865

iScience

CellPress
OPEN ACCESS

Article

SENP1 facilitates OM-MSC differentiation through activating OPTN-mediated mitophagy to mitigate the neurologic impairment following ICH

Jun He,[1] Jun Peng,[1] You Li,[1] Junwen Jiang,[1] Jiameng Li,[1] Long Lin,[1] Jian Wang,[1] and Ying Xia[1,2,*]

SUMMARY

Previous studies have indicated the neuroprotective effect of olfactory mucosa mesenchymal stem cells (OM-MSCs) on brain injury. Intracerebral hemorrhage (ICH) models were established in rats by injecting autologous blood. SENP1 expression was enhanced in neurons but decreased in astrocytes compared to that in OM-MSCs. Overexpression of SENP1 promoted the proliferation and neuronal differentiation, while inhibiting the astrocytic differentiation of OM-MSCs. Conversely, its knockdown had the opposite effect. Moreover, OM-MSCs reduced neurological dysfunction in rats after ICH, and the neuroprotective effect of OM-MSCs could be further enhanced by SENP1 overexpression. In addition, SENP1 promoted mitophagy, which might be related to SENP1-mediated OPTN deSUMOylation. Furthermore, SENP1 promoted neuronal differentiation of OM-MSCs through mitophagy mediated by OPTN. Similar to SENP1, OPTN transfection further enhanced the remission effect of OM-MSC on ICH rats. SENP1 promoted neuronal differentiation of OM-MSCs through OPTN-mediated mitophagy to improve neurological deficits in ICH rats.

INTRODUCTION

Intracerebral hemorrhage (ICH) is a severe and fatal subtype of stroke, accounting for about 10%–15% of all stroke cases, with high morbidity and mortality.[1] The sudden rupture of the cerebral blood vessel forms a large hematoma, which causes mechanical compression of the surrounding brain tissue, leading to intracranial hypertension and deterioration of nerve function.[2] However, surgical intervention for hematoma in patients with ICH rarely improves neurological outcomes.[3] Therefore, it is of great clinical significance to identify a target for the prevention and improvement of ICH.

Mesenchymal stem cells (MSCs) from bone marrow,[4] adipose tissue,[5] umbilical cord blood,[6] umbilical cord tissue,[7] and other sources have been used in the treatment of ICH. Previous meta-analyses have shown that stem cell therapy could significantly improve behavioral outcomes in animal models of ICH.[8] Olfactory mucosa (OM)-MSCs are located in the lamina propria of the nose, and they have a strong application value because they are relatively easy to obtain and are well suited for autologous transplantation.[9] Moreover, OM-MSCs have the ability of multidirectional differentiation and promote nervous system regeneration *in vivo*.[10] The therapeutic effect of OM-MSCs on ICH has been confirmed in related studies.[11] However, it is unclear whether OM-MSCs are targeted to differentiate into functional nerve cells and the underlying mechanism regulating OM-MSC differentiation. Understanding this mechanism might provide new ideas for solving clinical problems related to ICH.

SUMOylation is a reversible post-translational process implicated in transcriptional regulation through chromatin remodeling and modification of transcription factors.[12] The modification of SUMO leads to changes in the stability, activity, localization, or interaction of its substrates, which can affect cellular processes such as cell-cycle progression, DNA repair, and transport maintenance.[13] In addition, it has been suggested that SUMOylation is involved in the pathophysiological process of ischemic brain injury through the regulation of mitochondrial homeostasis, apoptotic signaling proteins, and oxidative stress.[14] SENP1, SUMO-specific protease 1, plays a neuroprotective role in ischemia/reperfusion (I/R) injury by suppressing neuronal apoptosis.[15] Moreover, SENP1-mediated Sirtuin 3 (Sirt3) deSUMOylation plays a crucial role in protecting the brain from I/R injury induced by selective intra-arterial cooling (SI-AC).[16] Optineurin (OPTN), the mitophagy receptor, has previously been reported as a potential therapeutic target for neurodegenerative diseases.[17] Interestingly, it was reported that some lysine residues of OPTN had SUMOylation sites.[18] However, it is unclear whether SENP1 influences OM-MSC differentiation during ICH progression through deSUMOylation of OPTN.

The current study aimed to elucidate the possible therapeutic effect of OM-MSCs during ICH progression and the regulatory role of SENP1 in OPTN-mediated mitophagy and OM-MSC neuronal differentiation. We hypothesized that SENP1 enhances OM-MSC neuronal

[1]Department of Neurosurgery, Haikou Affiliated Hospital of Central South University Xiangya School of Medicine, Haikou 570208, Hainan Province, P.R. China
[2]Lead contact
*Correspondence: xiaying0509@163.com
https://doi.org/10.1016/j.isci.2024.109865

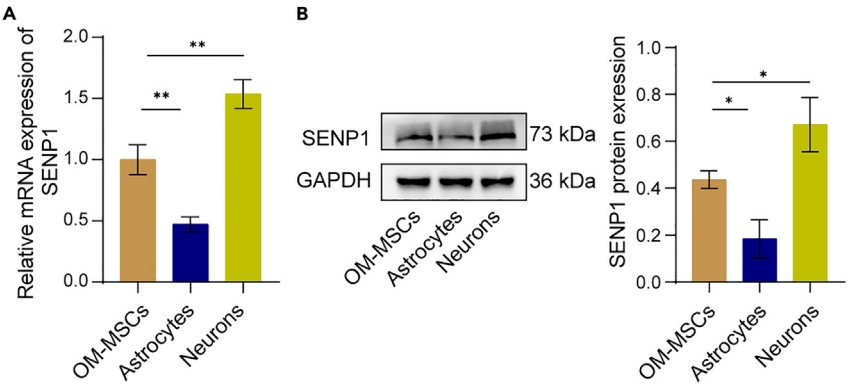

Figure 1. Dynamic levels of SENP1 during OM-MSC differentiation

(A and B) qPCR and western blot were utilized to measure SENP1 level in OM-MSCs, astrocytes, and neurons. Data are represented as means ± SD. Statistical difference was determined using one-way analysis of variance test followed by Tukey multiple-comparison post hoc analysis. $n = 3$. *$p < 0.05$, **$p < 0.01$.

differentiation through mitophagy in an OPTN-dependent manner to alleviate ICH. Our findings provided evidence that SENP1 is a potent therapy for ICH treatment.

RESULTS

Dynamic levels of SENP1 during OM-MSC differentiation

To investigate the potential role of SENP1 in OM-MSCs, we assessed the levels of SENP1 in OM-MSCs, astrocytes, and neurons. Among them, astrocytes and neurons are the outcomes of OM-MSCs-induced differentiation. As shown, SENP1 mRNA expression was increased in neurons and decreased in astrocytes compared to that in OM-MSCs (Figure 1A). Similarly, the SENP1 protein level was upregulated in neurons but downregulated in astrocytes (Figure 1B). These results imply that SENP1 might play a crucial role in the neural differentiation of OM-MSCs.

SENP1 facilitates the neuronal differentiation of OM-MSCs

The functional effect of SENP1 on neurogenesis was further evaluated in OM-MSCs. We overexpressed or knocked down SENP1 in OM-MSCs and assessed SENP1 levels using qPCR and western blot analysis (Figures 2A and 2B). Addition of SENP1 accelerated proliferation, whereas inhibition of SENP1 impeded proliferation in OM-MSCs (Figure 2C). Furthermore, the addition of SENP1 increased $NeuN^+$ cells and decreased $GFAP^+$ cells. Depletion of SENP1 increased $GFAP^+$ cells and reduced $NeuN^+$ cells (Figure 2D). Thus, these observations demonstrate that overexpression of SENP1 accelerates proliferation and neuronal differentiation in OM-MSCs.

SENP1 promotes OM-MSC neuronal differentiation to alleviate ICH-induced nerve damage

We established a rat model to explore the effect of SENP1-modified OM-MSCs on nerve injury after ICH and to identify the potential regulatory mechanism. As shown in Figures 3A–3D, ICH rats exhibited increased brain water content, decreased Garcia score, lower left forelimb placement rate, and decreased left turn rate at 24 and 72 h after ICH, suggesting neural function in ICH rats were damaged. The OM-MSC treatment significantly improved the impaired neurological function in ICH rats. Moreover, the overexpression of SENP1 enhanced the improvement of OM-MSCs in neurological impairment. Among them, the remission effect was more pronounced after 72 h of ICH. Based on the abovementioned results, ICH induction for 72 h was used for follow-up experiments. The apoptosis and degeneration of neurons after 72 h of ICH were observed using TUNEL and FJC staining. Compared with sham group, the number of TUNEL- and FJC-positive cells increased significantly in the ICH group. In addition, OM-MSCs could partially offset the promoting effect of ICH on neurodegeneration, and OM-MSCs transfected with oe-SENP1 have a more significant inhibitory effect on ICH-caused neurodegeneration (Figures 3E and 3F). Overexpression of SENP1 also enhanced the increase of NeuN fluorescent intensity and protein levels (Figures 3G and 3H) and the decrease of GFAP level induced by OM-MSCs (Figure 3H). Overall, SENP1 might promote OM-MSC neuronal differentiation to alleviate nerve damage at post-ICH.

Addition of SENP1 accelerates mitophagy

To determine the role of SENP1 in mitophagy, we evaluated the effect of overexpression or depletion of SENP1 on the levels of mitophagy-associated proteins. Addition of SENP1 enhanced LC3 II protein expression and decreased p62 protein levels in the cytoplasm and mitochondria. The knockout of SENP1 had opposite effects on the levels of LC3 II and p62 protein (Figure 4A). Moreover, the overexpression of SENP1 led to a significant increase in autophagosomes and their colocalization with mitochondria, whereas the deletion of SENP1 resulted in the opposite effect (Figure 4B). Briefly, the abovementioned data indicate that SENP1 facilitates mitophagy.

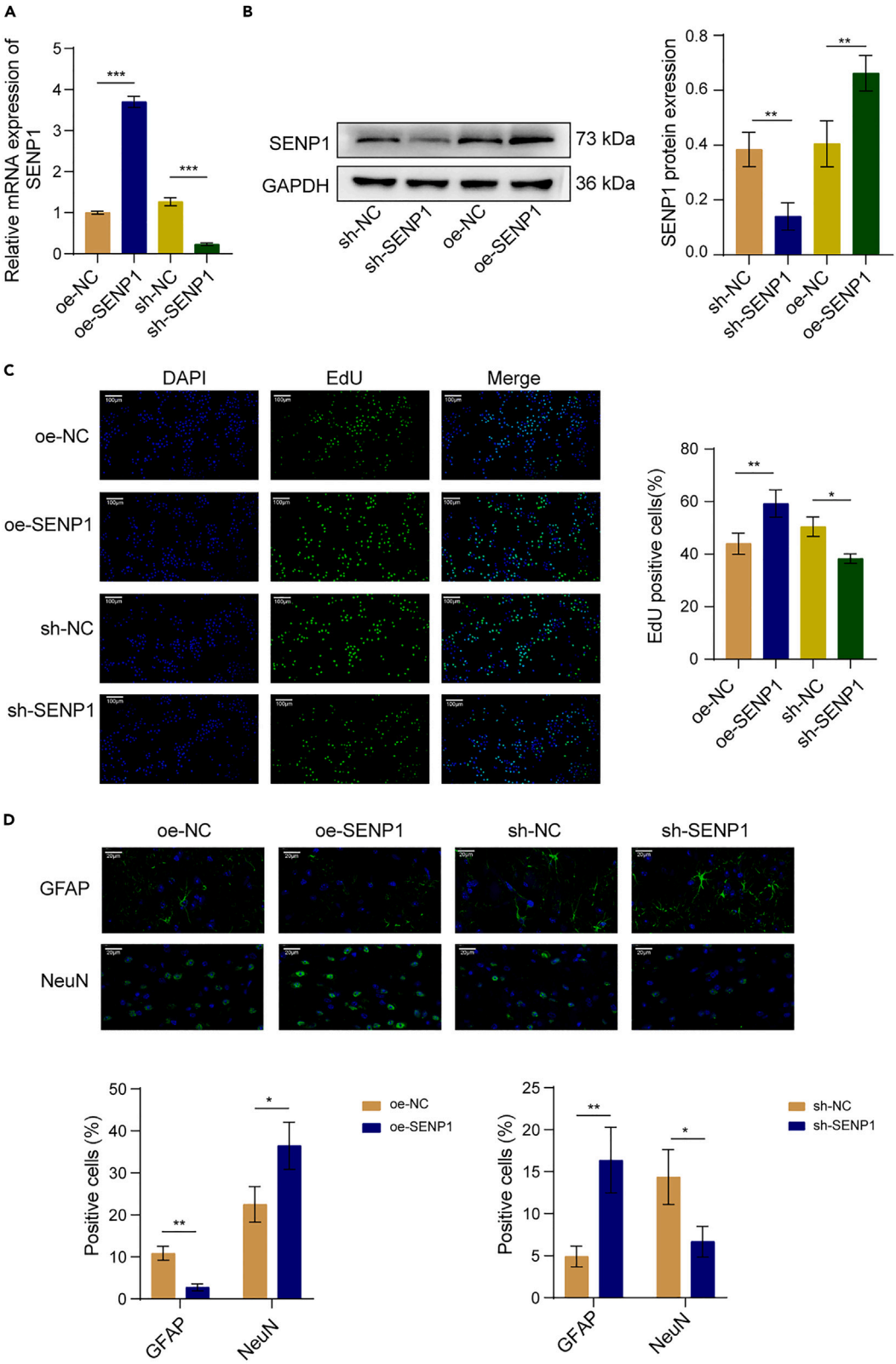
A
Relative mRNA expression of SENP1
oe-NC
oe-SENP1
sh-NC
sh-SENP1
B
SENP1
GAPDH
73 kDa
36 kDa
SENP1 protein exression
C
DAPI
EdU
Merge
EdU positive cells(%)
D
GFAP
NeuN
Positive cells (%)

Figure 2. SENP1 facilitates the neuronal differentiation of OM-MSCs

(A and B) qPCR and western blot were used to assess SENP1 level in OM-MSCs transfected with oe-NC, oe-SENP1, sh-NC, or sh-SENP1.

(C) EdU staining (scale bar, 100 μm) was performed to detect cell proliferation in OM-MSCs transfected with oe-NC, oe-SENP1, sh-NC, or sh-SENP1.

(D) The effect of SENP1 on $GFAP^+$ cells and $NeuN^+$ cells was assessed by IF staining (scale bar, 20 μm). Data are represented as means ± SD. Statistical analysis of the data from two groups was performed using Student's t test. $n = 3$. $^*p < 0.05$, $^{**}p < 0.01$, $^{***}p < 0.001$.

SENP1 regulates mitophagy by controlling the SUMOylation of OPTN

Previous studies have shown that OPTN-mediated mitochondrial autophagy restrains secondary brain injury and NLRP3 inflammasome activation after ICH.[19] We speculated that SENP1 might affect mitophagy by regulating OPTN. We first learned through western blot that overexpression of SENP1 increased the OPTN protein level, whereas silencing of SENP1 decreased the OPTN protein level (Figure 5A). SUMOylation of NCX3 by SUMO1 was involved in neuroprotection induced by ischemic preconditioning.[20] SENP1 regulates neuroinflammation by deSUMOylating NEMO and modulating of its stability.[21] Here, we observed that the level of SUMO1 was declined after SENP1 overexpression and enhanced after SENP1 silencing, suggesting SENP1-mediated SUMO modification of OPTN (Figure 5B). Moreover, the effect of OPTN on mitochondria was similar to that of SENP1. The overexpression of OPTN promoted mitophagy, whereas the knockdown had the opposite effect (Figures 5C and 5D). These results revealed that SENP1 overexpression promotes mitophagy, which might be related to the decreased amount of SUMOylated OPTN.

SENP1 accelerates OM-MSC neuronal differentiation through regulating OPTN

The EdU assay indicated that SENP1 knockdown could abolish the promotive effect of OPTN abundance on the proliferation of OM-MSCs, whereas overexpression of SENP1 could alleviate the repressive effect of OPTN depletion on the proliferation of OM-MSCs (Figure 6A). Moreover, OPTN abundance increased $NeuN^+$ cells and decreased $GFAP^+$ cells, but this effect was counteracted by SENP1 silencing. OPTN depletion increased the number of $GFAP^+$ cells and decreased the number of $NeuN^+$ cells, but overexpression of SENP1 attenuated these effects (Figure 6B). Taken together, the promotion effect of SENP1 on OM-MSC neuronal differentiation is associated with OPTN.

OPTN promotes OM-MSC neuronal differentiation to ameliorate ICH-caused nerve damage

To investigate the effects of OPTN-treated OM-MSCs on ICH, ICH rats were respectively assigned to sham, ICH, ICH + OM-MSCs, ICH + OM-MSCs oe-NC, and ICH + OM-MSCs oe-OPTN groups. Distinct neurological deficits were found in the ICH group at 24 h and 72 h compared to the sham group. Treatment with OM-MSCs remarkably improved neurological outcomes 72 h post-ICH, and oe-OPTN could further enhance the beneficial effects of OM-MSCs (Figures 7A–7D). Similarly, OM-MSCs significantly improved the neurodegeneration caused by ICH, as evidenced by the decrease in TUNEL and FJC-positive cells. Transfection with oe-OPTN further enhanced the beneficial effects of OM-MSCs (Figures 7E and 7F). Furthermore, in the ICH group, NeuN fluorescent intensity and protein level (Figures 7G and 7H) and LC3 II protein level declined, whereas GFAP and p62 protein levels elevated, which was partly reversed after OM-MSCs treatment. Moreover, further transfection with oe-OPTN enhanced the therapeutic effect of OM-MSCs (Figure 7H). Taken together, OPTN increased mitophagy and OM-MSC neuronal differentiation to improve nerve damage post-ICH.

DISCUSSION

Neurogenesis is a crucial process in brain repair after ICH, and boosting these processes can accelerate recovery. Zhou et al. indicated that Compound K potentiated the neurogenesis of endogenous neural stem cells after thrombin stimulation. The results showed an improved behavioral prognosis after ICH in mice.[22] Chen et al. introduced a novel approach to enhance endogenous neurogenesis and mitigate partial neural deficits by activating Notch1 signaling in ICH.[23] Therefore, an in-depth exploration of the underlying mechanism of post-ICH neurogenesis may be an important approach to enhance the prognosis of ICH. Moreover, activation of mitophagy could reduce the damage caused by traumatic brain injury and improve neurological dysfunction.[24] Zheng et al. illustrated that the FUN14 domain-containing 1 (FUNDC1) protein inhibited NLRP3-regulated inflammation by promoting mitophagy after ICH in mice.[25] Scalp acupuncture alleviated brain injury after ICH in rats by enhancing mitophagy and reducing apoptosis.[26] Therefore, this study aimed to investigate the potential mechanisms regulating neurogenesis and mitophagy after ICH, with the goal of offering novel insights for the treatment of ICH.

The protective effect of SENP1 has been proven in a variety of cerebrovascular diseases. For instance, SENP1 protects neurons from apoptosis during transient cerebral I/R.[15] In mice after brain ischemia, the absence of SENP1 in pericytes could worsen ischemic injury and speed up thrombosis.[27] Therefore, we hypothesize that SENP1 might play a key role in ICH, and further exploration is needed to understand the underlying mechanism of SENP1's role. Liu et al. highlighted out the neuroprotective effect of OM-MSCs in ICH models and found that hypoxia preconditioning improved the survival of OM-MSCs in the ICH microenvironment by inducing miR-326/polypyrimidine tract-binding protein 1 (PTBP1)/PI3K-regulated autophagy.[28] Moreover, OM-MSCs have the potential to differentiate into neurons, bone cells, smooth muscle cells, and adipocytes.[29] If SENP1 plays an important role in the neuronal differentiation of OM-MSCs, it might offer new insights for the treatment of ICH. In this study, we observed that SENP1 was increased in neurons and decreased in astrocytes compared to OM-MSCs, implying that SENP1 is closely related to neural differentiation. Moreover, the addition of SENP1 stimulated OM-MSC proliferation, enhanced $NeuN^+$ cells, and decreased $GFAP^+$ cells. SENP1 depletion restrained OM-MSC proliferation, increased the number of $GFAP^+$ cells, and reduced the number of $NeuN^+$ cells. Furthermore, we demonstrated through experiments that SENP1-overexpressed OM-MSCs alleviate neural damage after ICH.

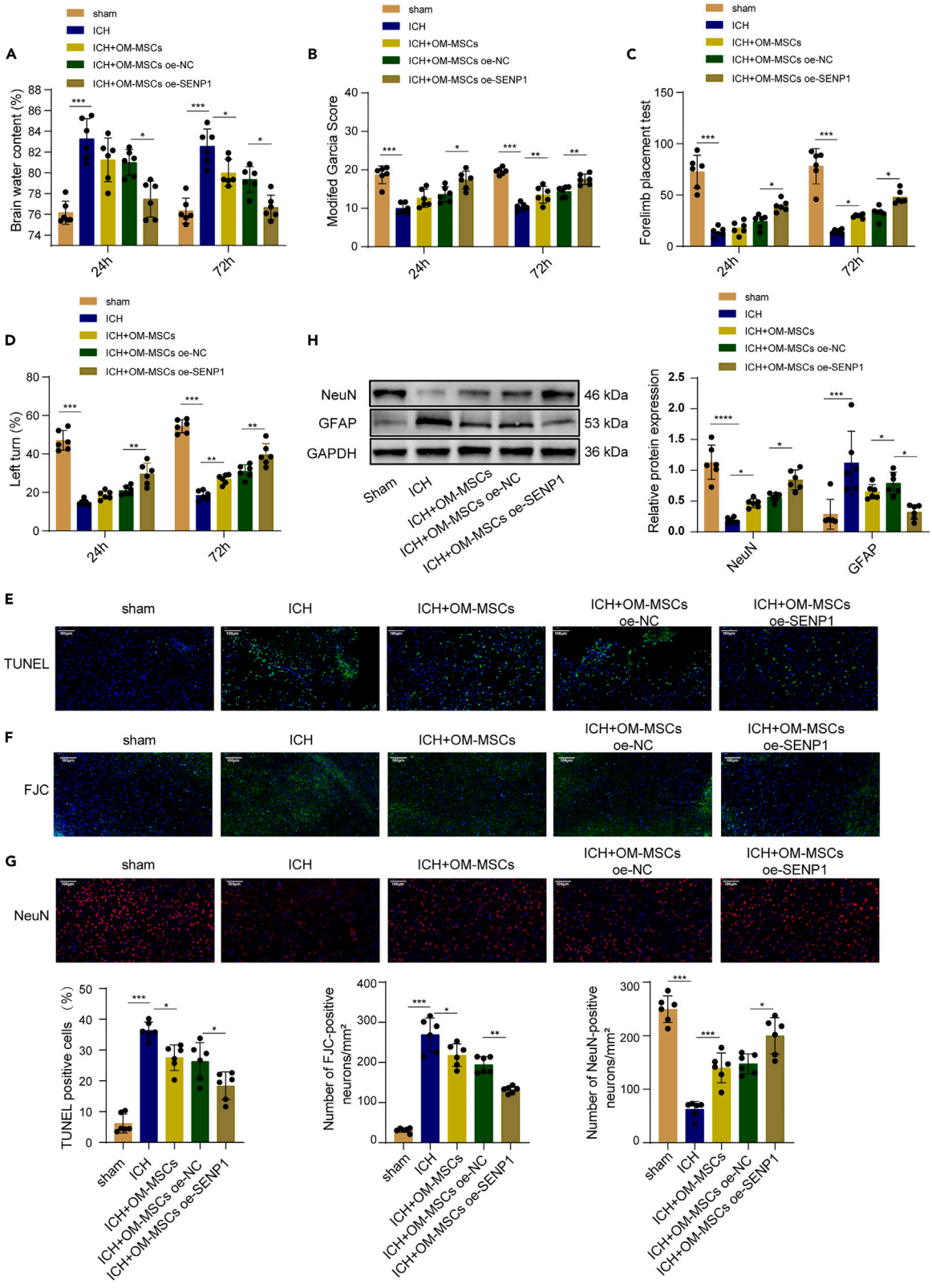
A
B
C
D
E
F
G
H
sham
ICH
ICH+OM-MSCs
ICH+OM-MSCs oe-NC
ICH+OM-MSCs oe-SENP1
Brain water content (%)
Modified Garcia Score
Forelimb placement test
Left turn (%)
24h
72h
NeuN
GFAP
GAPDH
46 kDa
53 kDa
36 kDa
Relative protein expression
TUNEL
FJC
TUNEL positive cells (%)
Number of FJC-positive neurons/mm²
Number of NeuN-positive neurons/mm²

Figure 3. SENP1 promotes OM-MSC neuronal differentiation to alleviate ICH-induced nerve damage

(A) Analysis of brain water content in brain region at 24 h and 72 h after ICH, which were performed in rats in sham, ICH, ICH + OM-MSCs, ICH + OM-MSCs oe-NC, and ICH + OM-MSCs oe-SENP1 groups.

(B) Modified Garcia test, (C) forelimb placement test, and (D) corner turn test were detected at 24 h and 72 h after ICH.

(E and F) Representative images of TUNEL and FJC in the perihematoma area at 72 h after ICH (scale bar, 100 μm).

(G) Representative IF staining with NeuN in the perihematoma area at 72 h after ICH (scale bar, 100 μm).

(H) Western blot was utilized to measure NeuN and GFAP protein levels. Data are represented as means ± SD. Statistical difference among multiple groups was determined using one-way analysis of variance test followed by Tukey multiple-comparison post hoc analysis. $n = 6$. *$p < 0.05$, **$p < 0.01$, ***$p < 0.001$.

Studies have shown that mitophagy is a selective form of autophagy that can eliminate damaged mitochondria. It is an integral part of mitochondrial quality control.[25] The dysfunctional mitochondria are enveloped by the autophagosome and fused with the lysosome to complete a series of degradation processes. According to studies, scalp acupuncture could reduce brain damage in rats with ICH by enhancing mitochondrial autophagy and reducing apoptosis and inflammatory response.[26] Here, the overexpression of SENP1 led to an upregulation of cytoplasmic and mitochondrial LC3 II levels and a downregulation of p62 levels. Depletion of SENP1 has the opposite effect. Also, SENP1 improved the co-localization of GFP-LC3 and MitoTracker, whereas SENP1 knockout had the opposite effect on the degree of co-localization. These results suggest that SENP1 promotes mitophagy in OM-MSCs.

SUMOylation is involved in a wide range of essential protein modifications for cellular processes such as transcription, signal transduction, genome integrity, and nuclear transport.[30] SUMOylation can be catalyzed by SUMO-specific activation, coupling, and ligase.[31] SENP1 is the

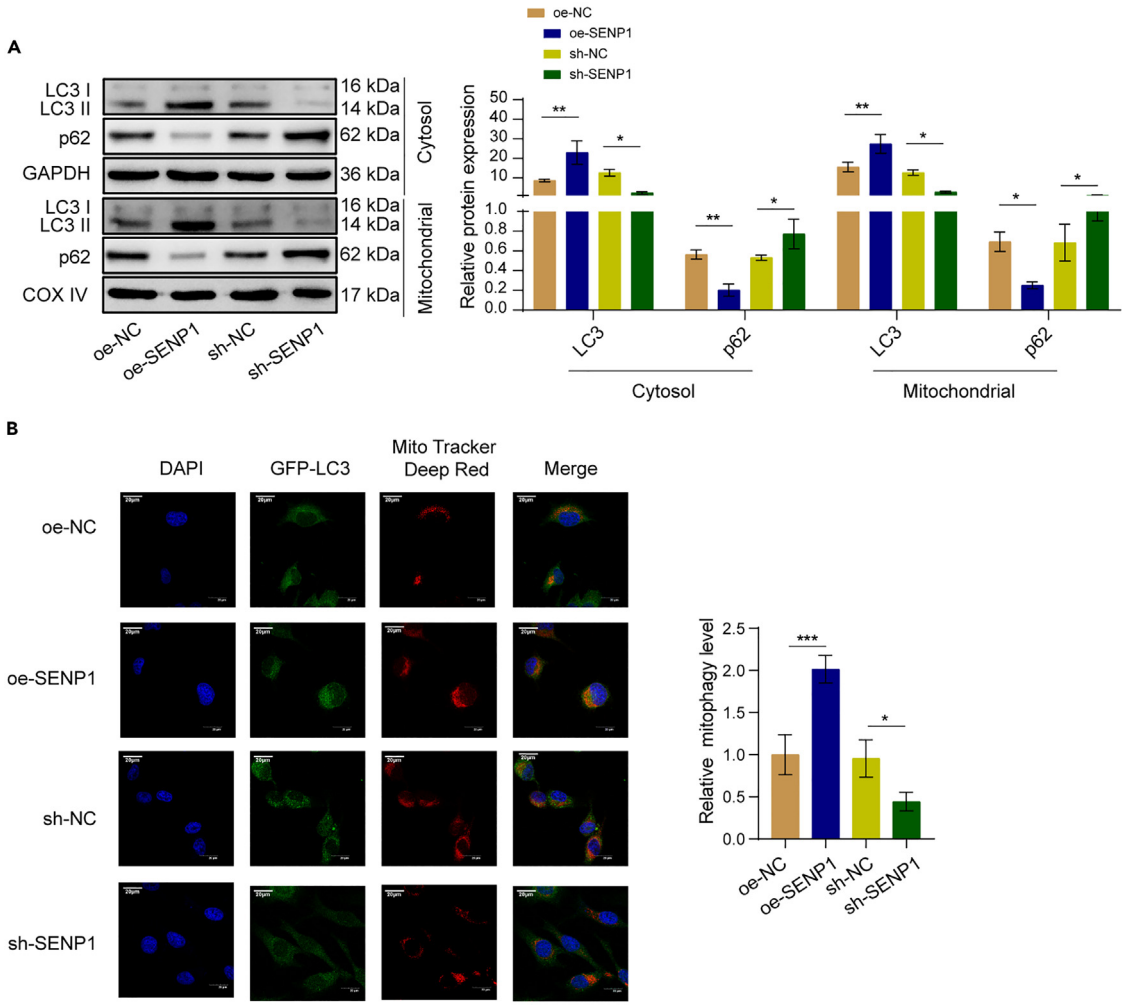

Figure 4. Addition of SENP1 accelerates mitophagy

(A) Western blot was used to measure the protein levels of LC3 and p62.

(B) Mitochondria (Mito Tracker Deep Red) and GFP-LC3 (green) colocalization were detected using confocal microscopy (scale bar, 20 μm). Data are represented as means ± SD. Statistical analysis of the data from two groups was performed using Student's t test. $n = 3$. *$p < 0.05$, **$p < 0.01$, ***$p < 0.001$.

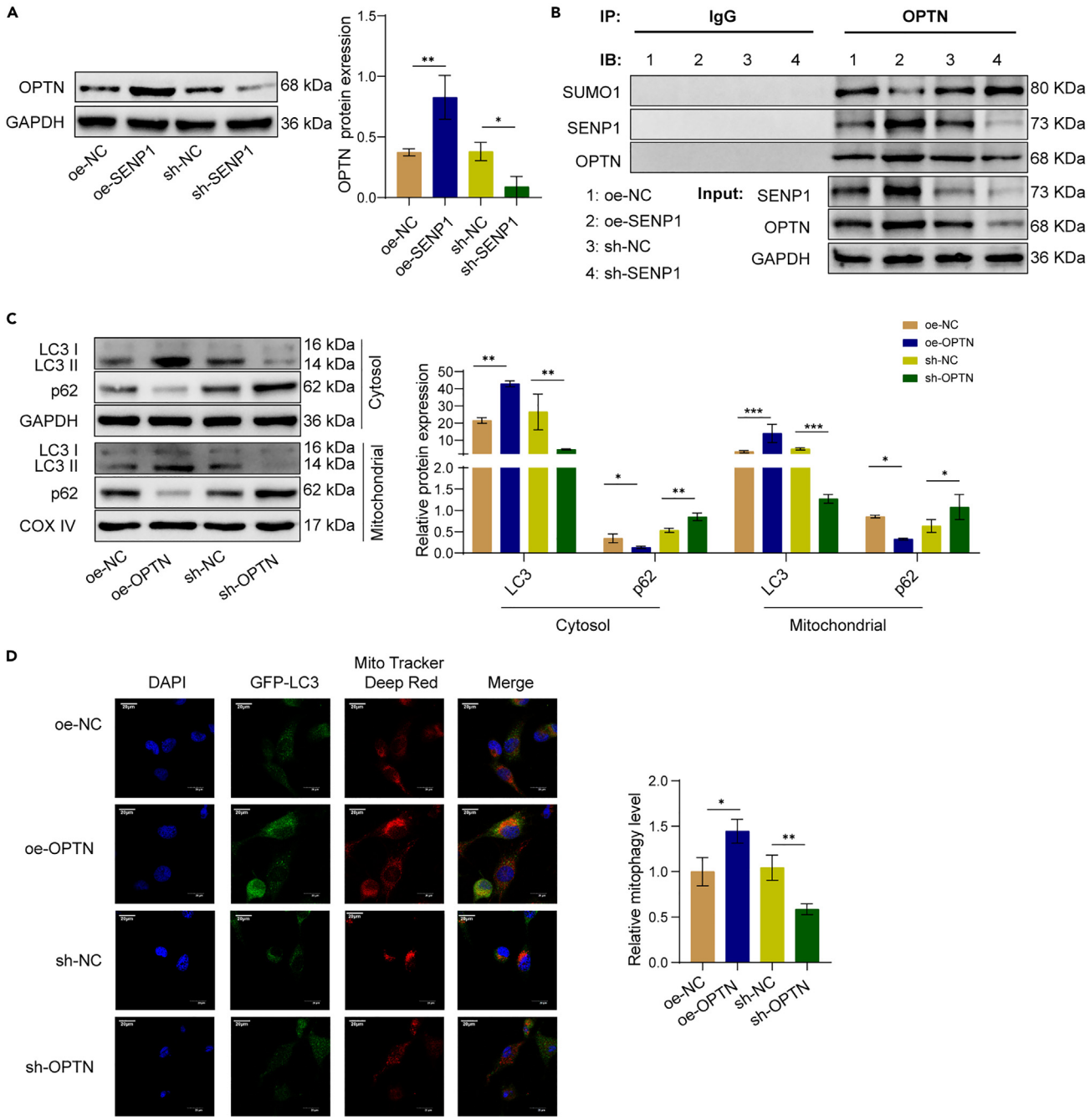

Figure 5. SENP1 regulates mitophagy by controlling the SUMOylation of OPTN

(A) Western blot was utilized to assess OPTN level.

(B) SUMOylation modification analysis was performed to identify the levels of OPTN SUMOylation in SENP1 overexpression and knockdown cells.

(C) Western blot was used to measure the protein levels of LC3 and p62.

(D) Mitochondria (Mito Tracker Deep Red) and GFP-LC3 (green) colocalization were detected using confocal microscopy (scale bar, 20 μm). Data are represented as means ± SD. Statistical analysis of the data from two groups was performed using Student's t test. $n = 3$. *$p < 0.05$, **$p < 0.01$, ***$p < 0.001$.

first SUMO-specific protease to be discovered and is involved in a variety of diseases.[32] SENP1 regulated the deSUMOylation of NEMO, suppressing microglial inflammation induced by intermittent hypoxia.[33] Moreover, one finding suggested that OPTN SUMOylation is well conserved in mammals.[18] Based on this, we speculated that SENP1 might influence ICH through the deSUMOylation of OPTN. Consistent with the predicted results, the addition of SENP1 increased the expression of OPTN and decreased the SUMOylation of OPTN. Depletion

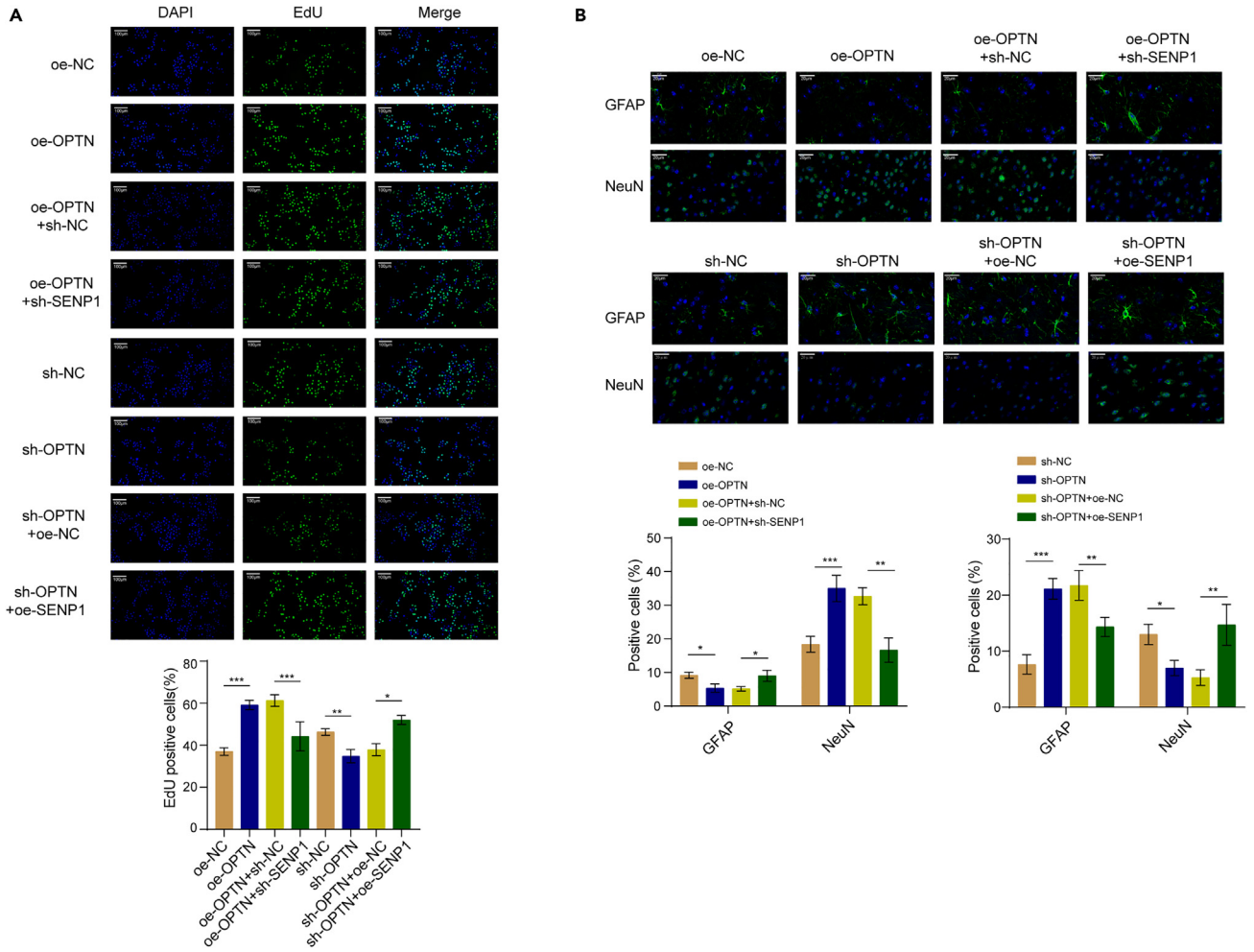

Figure 6. SENP1 accelerates OM-MSC neuronal differentiation through regulating OPTN

OM-MSCs transfected with oe-NC, oe-OPTN, oe-OPTN + sh-NC, oe-OPTN + sh-SENP1, sh-NC, sh-OPTN, sh-OPTN + oe-NC, or sh-OPTN + oe-SENP1.

(A) EdU staining (scale bar, 100 μm) was performed to detect cell proliferation.

(B) The expressions of GFAP and NeuN were observed by IF staining (scale bar, 20 μm). Data are represented as means ± SD. Statistical difference among multiple groups was determined using one-way analysis of variance test followed by Tukey multiple-comparison post hoc analysis. $n = 3$. $^{*}p < 0.05$, $^{**}p < 0.01$, $^{***}p < 0.001$.

of SENP1 decreased OPTN expression and enhanced the SUMOylation of OPTN. Previous studies have indicated that OPTN-regulated mitochondrial autophagy inhibits NLRP3 inflammasome activation after ICH.[34] In this study, OPTN promoted mitophagy and inhibited it after knockdown. Moreover, SENP1 promoted OM-MSC neuron differentiation through mitophagy mediated by OPTN. Furthermore, OM-MSCs transfected with OPTN overexpression plasmid alleviated nerve damage after ICH.

We reported that SENP1 effectively facilitated OM-MSC neuron differentiation to alleviate neurological damage after ICH. Moreover, our data also showed that SENP1 promoted mitophagy by regulating the SUMOylation of OPTN. Furthermore, OPTN could also promote OM-MSC neuronal differentiation to alleviate nerve damage after ICH. Based on the current study, we propose SENP1 as an attractive treatment strategy for ICH.

Limitations of the study

Our research has certain limitations to a certain extent. The regulatory mechanism of SENP1 in alleviating nerve injury after ICH needs further exploration, potentially involving not only the regulation of OPTN. Furthermore, we did not study the regulatory mechanisms upstream of SENP1. These limitations will guide our future research directions.

STAR★METHODS

Detailed methods are provided in the online version of this paper and include the following:

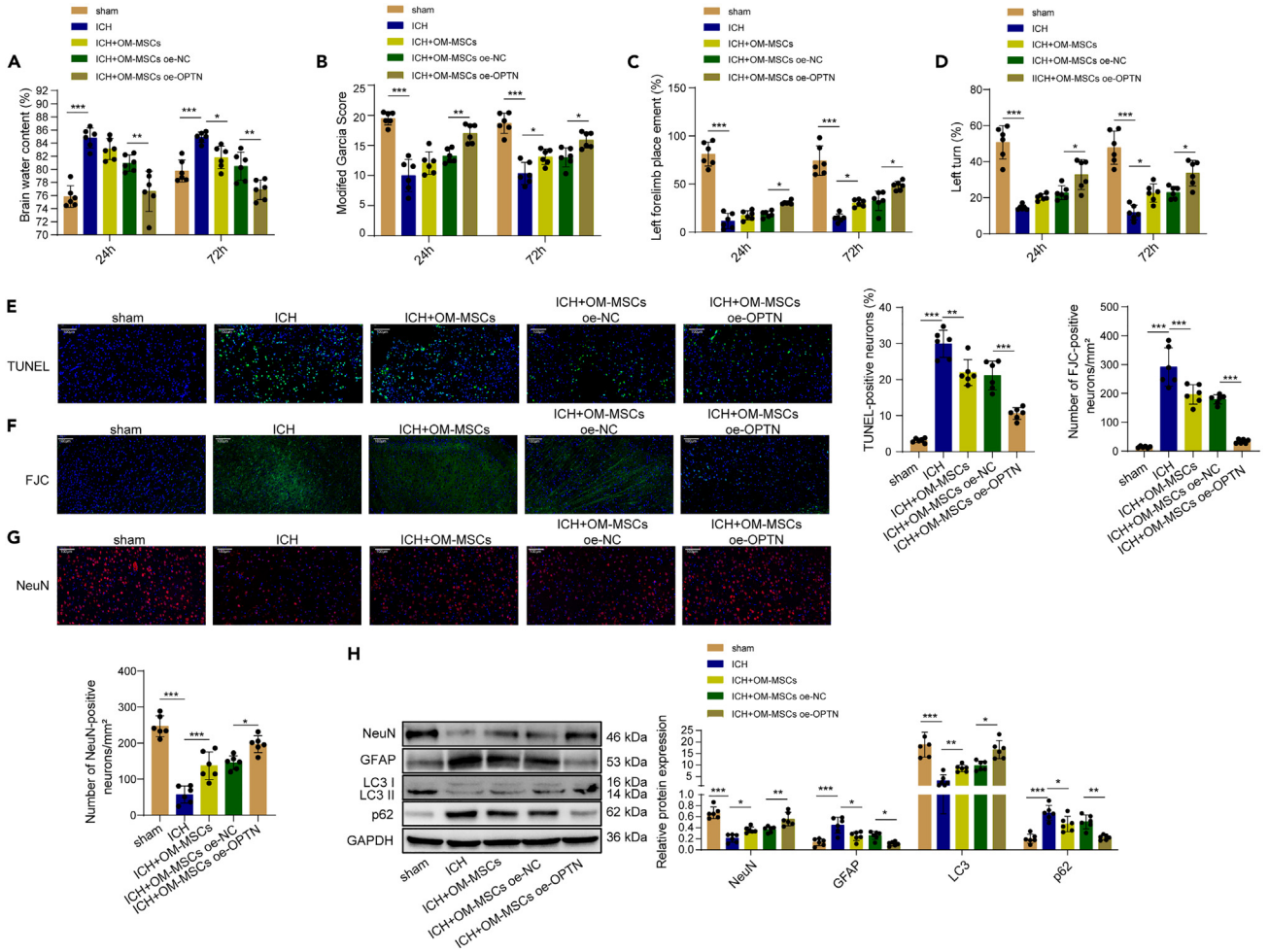

Figure 7. OPTN increases OM-MSC neuronal differentiation to ameliorate ICH-caused nerve damage

(A) The neurological severity was assessed via brain water content, (B) modified Garcia test, (C) forelimb placement test, and (D) corner turn test, which were performed in the sham, ICH, ICH + OM-MSCs, ICH + OM-MSCs oe-NC, and ICH + OM-MSCs oe-OPTN groups at 24 and 72 h after ICH.

(E and F) Representative images of TUNEL (scale bar, 100 μm) and FJC (scale bar, 100 μm) in the perihematoma area at 72 h after ICH.

(G) IF staining of NeuN was performed in the perihematoma area at 72 h after ICH (scale bar, 100 μm).

(H) Western blot was utilized to assess NeuN, GFAP, LC3, and p62 protein levels. Data are represented as means ± SD. Statistical difference among multiple groups was determined using one-way analysis of variance test followed by Tukey multiple-comparison post hoc analysis. $n = 6$. *$p < 0.05$, **$p < 0.01$, ***$p < 0.001$.

- Immunofluorescence
- TUNEL staining
- Fluoro-Jade C (FJC) staining
- 5-Ethynyl-2′-deoxyuridine (EdU) staining
- Western blot
- Immunoprecipitation (IP)
- qPCR assay
- Mitophagy evaluation

- QUANTIFICATION AND STATISTICAL ANALYSIS

ACKNOWLEDGMENTS

We would like to thank the anonymous reviewers who have helped to improve the paper. This work was supported by the Special Project of Clinical Medical Research Center for Cerebrovascular Disease of Hainan Province (LCYX202309).

AUTHOR CONTRIBUTIONS

Y.X. guaranteed the integrity of the entire study; J.H. and J.P. designed the study and literature research; Y.X. defined the intellectual content; Y.L. and J.J. performed experiment; J.L. and L.L. collected the data; J.W. analyzed the data; Y.X. wrote the main manuscript and prepared figures. All authors reviewed the manuscript.

DECLARATION OF INTERESTS

The authors declare that they have no known competing financial interests or personal relationships that could have appeared to influence the work reported in this paper.

Received: January 16, 2024
Revised: April 2, 2024
Accepted: April 27, 2024
Published: April 30, 2024

REFERENCES

1. Keep, R.F., Hua, Y., and Xi, G. (2012). Intracerebral haemorrhage: mechanisms of injury and therapeutic targets. Lancet. Neurol. *11*, 720–731. https://doi.org/10.1016/S1474-4422(12)70104-7.
2. Bautista, W., Adelson, P.D., Bicher, N., Themistocleous, M., Tsivgoulis, G., and Chang, J.J. (2021). Secondary mechanisms of injury and viable pathophysiological targets in intracerebral hemorrhage. Ther. Adv. Neurol. Disord. *14*, 17562864211049208. https://doi.org/10.1177/17562864211049208.
3. Dey, M., Stadnik, A., and Awad, I.A. (2014). Spontaneous intracerebral and intraventricular hemorrhage: advances in minimally invasive surgery and thrombolytic evacuation, and lessons learned in recent trials. Neurosurgery *74*, S142–S150. https://doi.org/10.1227/NEU.0000000000000221.
4. Chen, M., Li, X., Zhang, X., He, X., Lai, L., Liu, Y., Zhu, G., Li, W., Li, H., Fang, Q., et al. (2015). The inhibitory effect of mesenchymal stem cell on blood-brain barrier disruption following intracerebral hemorrhage in rats: contribution of TSG-6. J. Neuroinflammation *12*, 61. https://doi.org/10.1186/s12974-015-0284-x.
5. Zhang, Y., Deng, H., Hu, Y., Pan, C., Wu, G., Li, Q., and Tang, Z. (2019). Adipose-derived mesenchymal stem cells stereotactic transplantation alleviate brain edema from intracerebral hemorrhage. J. Cell. Biochem. *120*, 14372–14382. https://doi.org/10.1002/jcb.28693.
6. Kim, K., Park, H.W., Moon, H.-E., Kim, J.W., Bae, S., Chang, J.W., Oh, W., Yang, Y.S., and Paek, S.H. (2015). The effect of human umbilical cord blood-derived mesenchymal stem cells in a collagenase-induced intracerebral hemorrhage rat model. Exp. Neurobiol. *24*, 146–155.
7. Mello, T.G., Rosado-de-Castro, P.H., Vasques, J.F., Pinhão, C., Santos, T.M., de Lima, R.R., Foerster, B.U., Paiva, F.F., Mendez-Otero, R., and Pimentel-Coelho, P.M. (2022). Hyperacute transplantation of umbilical cord mesenchymal stromal cells in a model of severe intracerebral hemorrhage. Future Sci. OA *8*, FSO793.
8. Hu, Y., Liu, N., Zhang, P., Pan, C., Zhang, Y., Tang, Y., Deng, H., Aimaiti, M., Zhang, Y., Zhou, H., et al. (2016). Preclinical Studies of Stem Cell Transplantation in Intracerebral Hemorrhage: a Systemic Review and Meta-Analysis. Mol. Neurobiol. *53*, 5269–5277. https://doi.org/10.1007/s12035-015-9441-6.
9. Nivet, E., Vignes, M., Girard, S.D., Pierrisnard, C., Baril, N., Devèze, A., Magnan, J., Lanté, F., Khrestchatisky, M., Féron, F., and Roman, F.S. (2011). Engraftment of human nasal olfactory stem cells restores neuroplasticity in mice with hippocampal lesions. J. Clin. Invest. *121*, 2808–2820. https://doi.org/10.1172/JCI44489.
10. Ge, L., Jiang, M., Duan, D., Wang, Z., Qi, L., Teng, X., Zhao, Z., Wang, L., Zhuo, Y., and Chen, P. (2016). Secretome of olfactory mucosa mesenchymal stem cell, a multiple potential stem cell. Stem Cells Int. *2016*, 1243659.
11. Liu, J., He, J., Huang, Y., Ge, L., Xiao, H., Zeng, L., Jiang, Z., Lu, M., and Hu, Z. (2021). Hypoxia-preconditioned mesenchymal stem cells attenuate microglial pyroptosis after intracerebral hemorrhage. Ann. Trans. Med. *9*, 1362.
12. Talamillo, A., Barroso-Gomila, O., Giordano, I., Ajuria, L., Grillo, M., Mayor, U., and Barrio, R. (2020). The role of SUMOylation during development. Biochem. Soc. Trans. *48*, 463–478.
13. Bernstock, J.D., Peruzzotti-Jametti, L., Leonardi, T., Vicario, N., Ye, D., Lee, Y.-J., Maric, D., Johnson, K.R., Mou, Y., Van Den Bosch, A., et al. (2019). SUMOylation promotes survival and integration of neural stem cell grafts in ischemic stroke. EBioMedicine *42*, 214–224.
14. Hochrainer, K. (2018). Protein modifications with ubiquitin as response to cerebral ischemia-reperfusion injury. Transl. Stroke Res. *9*, 157–173.
15. Zhang, H., Wang, Y., Zhu, A., Huang, D., Deng, S., Cheng, J., Zhu, M.X., and Li, Y. (2016). SUMO-specific protease 1 protects neurons from apoptotic death during transient brain ischemia/reperfusion. Cell Death Dis. *7*, e2484.
16. Cai, H., Bian, X., Chen, L., Zhang, N., Li, L., Tang, W., Liu, X., and Li, Z. (2021). Selective intra-arterial brain cooling induces cerebral protection against ischemia/reperfusion injury through SENP1-Sirt3 signaling. Free Radic. Biol. Med. *171*, 272–283.
17. He, L., Chen, L., and Li, L. (2017). The TBK1-OPTN axis mediates crosstalk between

mitophagy and the innate immune response: a potential therapeutic target for neurodegenerative diseases. Neurosci. Bull. *33*, 354–356.

18. Hu, X., and Wu, H. (2022). SUMOylation of optineurin is critical for inhibiting interferon β production. Biochem. Biophys. Res. Commun. *623*, 189–195.
19. Cheng, Y., Liu, M., Tang, H., Chen, B., Yang, G., Zhao, W., Cai, Y., and Shang, H. (2021). iTRAQ-Based Quantitative Proteomics Indicated Nrf2/OPTN-Mediated Mitophagy Inhibits NLRP3 Inflammasome Activation after Intracerebral Hemorrhage. Oxid. Med. Cell. Longev. *2021*, 6630281. https://doi.org/10.1155/2021/6630281.
20. Cuomo, O., Pignataro, G., Sirabella, R., Molinaro, P., Anzilotti, S., Scorziello, A., Sisalli, M.J., Di Renzo, G., and Annunziato, L. (2016). Sumoylation of LYS590 of NCX3 f-Loop by SUMO1 participates in brain neuroprotection induced by ischemic preconditioning. Stroke *47*, 1085–1093.
21. Wang, H., Yang, T., Sun, J., Zhang, S., and Liu, S. (2021). SENP1 modulates microglia-mediated neuroinflammation toward intermittent hypoxia-induced cognitive decline through the de-SUMOylation of NEMO. J. Cell. Mol. Med. *25*, 6841–6854.
22. Zhou, L., Yang, F., Yin, J.-W., Gu, X., Xu, Y., and Liang, Y.-Q. (2020). Compound K induces neurogenesis of neural stem cells in thrombin induced nerve injury through LXRα signaling in mice. Neurosci. Lett. *729*, 135007.
23. Chen, J., Yuan, X.-Y., and Zhang, X. (2021). Intracerebral hemorrhage influences hippocampal neurogenesis and neurological function recovery via Notch1 signaling. Neuroreport *32*, 489–497.
24. Luan, Y., Jiang, L., Luan, Y., Xie, Y., Yang, Y., and Ren, K.-D. (2023). Mitophagy and Traumatic Brain Injury: Regulatory Mechanisms and Therapeutic Potentials. Oxid. Med. Cell. Longev. *2023*, 1649842.
25. Zheng, S., Jian, D., Gan, H., Wang, L., Zhao, J., and Zhai, X. (2021). FUNDC1 inhibits NLRP3-mediated inflammation after intracerebral hemorrhage by promoting mitophagy in mice. Neurosci. Lett. *756*, 135967.
26. Liu, P., Yu, X., Dai, X., Zou, W., Yu, X., Niu, M., Chen, Q., Teng, W., Kong, Y., Guan, R., and Liu, X. (2021). Scalp acupuncture attenuates brain damage after intracerebral hemorrhage through enhanced mitophagy and reduced apoptosis in rats. Front. Aging Neurosci. *13*, 718631.
27. Sun, M., Chen, X., Yin, Y.X., Gao, Y., Zhang, L., Chen, B., Ji, Y., Fukunaga, K., Han, F., and Lu, Y.M. (2020). Role of pericyte-derived SENP1 in neuronal injury after brain ischemia. CNS Neurosci. Ther. *26*, 815–828.
28. Liu, J., He, J., Ge, L., Xiao, H., Huang, Y., Zeng, L., Jiang, Z., Lu, M., and Hu, Z. (2021). Hypoxic preconditioning rejuvenates mesenchymal stem cells and enhances neuroprotection following intracerebral hemorrhage via the miR-326-mediated autophagy. Stem Cell Res. Ther. *12*, 413. https://doi.org/10.1186/s13287-021-02480-w.
29. He, J., Liu, J., Huang, Y., Zhuo, Y., Chen, W., Duan, D., Tang, X., Lu, M., and Hu, Z. (2020). Olfactory mucosa mesenchymal stem cells alleviate cerebral ischemia/reperfusion injury via Golgi apparatus secretory pathway Ca2+-ATPase isoform1. Front. Cell Dev. Biol. *8*, 586541.
30. Wang, Q., Xia, N., Li, T., Xu, Y., Zou, Y., Zuo, Y., Fan, Q., Bawa-Khalfe, T., Yeh, E.T.H., and Cheng, J. (2013). SUMO-specific protease 1 promotes prostate cancer progression and metastasis. Oncogene *32*, 2493–2498.
31. Pascual, G., Fong, A.L., Ogawa, S., Gamliel, A., Li, A.C., Perissi, V., Rose, D.W., Willson, T.M., Rosenfeld, M.G., and Glass, C.K. (2005). A SUMOylation-dependent pathway mediates transrepression of inflammatory response genes by PPAR-γ. Nature *437*, 759–763.
32. Xu, Y., Li, J., Zuo, Y., Deng, J., Wang, L.-S., and Chen, G.-Q. (2011). SUMO-specific protease 1 regulates the *in vitro* and *in vivo* growth of colon cancer cells with the upregulated expression of CDK inhibitors. Cancer Lett. *309*, 78–84.
33. Yang, T., Sun, J., Wei, B., and Liu, S. (2020). SENP1-mediated NEMO de-SUMOylation inhibits intermittent hypoxia induced inflammatory response of microglia *in vitro*. J. Cell. Physiol. *235*, 3529–3538.
34. Cheng, Y., Liu, M., Tang, H., Chen, B., Yang, G., Zhao, W., Cai, Y., and Shang, H. (2021). iTRAQ-based quantitative proteomics indicated Nrf2/OPTN-mediated mitophagy inhibits NLRP3 inflammasome activation after intracerebral hemorrhage. Oxid. Med. Cell. Longev. *2021*, 6630281.
35. Wang, Z., Zhang, X., Qi, L., Feng, W., Gu, Y., and Ding, Y. (2022). Olfactory mucosa tissue-derived mesenchymal stem cells lysate ameliorates LPS-induced acute liver injury in mice. BMC Pulm. Med. *22*, 414.
36. Fan, J.R., Lee, H.T., Lee, W., Lin, C.H., Hsu, C.Y., Hsieh, C.H., and Shyu, W.C. (2018). Potential role of CBX7 in regulating pluripotency of adult human pluripotent-like olfactory stem cells in stroke model. Cell Death Dis. *9*, 502. https://doi.org/10.1038/s41419-018-0519-8.
37. Xu, B., Li, Q., Wu, Y., Wang, H., Xu, J., Liu, H., and Xuan, A. (2022). Mettl3-mediated m(6) A modification of Lrp2 facilitates neurogenesis through Ythdc2 and elicits antidepressant-like effects. Faseb. J. *36*, e22392. https://doi.org/10.1096/fj.202200133RR.
38. Zhao, M., Gao, J., Cui, C., Zhang, Y., Jiang, X., and Cui, J. (2021). Inhibition of PTEN ameliorates secondary hippocampal injury and cognitive deficits after intracerebral hemorrhage: Involvement of AKT/FoxO3a/ATG-mediated autophagy. Oxid. Med. Cell. Longev. *2021*, 5472605.
39. Zhou, Y., Wang, S., Li, Y., Yu, S., and Zhao, Y. (2017). SIRT1/PGC-1α signaling promotes mitochondrial functional recovery and reduces apoptosis after intracerebral hemorrhage in rats. Front. Mol. Neurosci. *10*, 443.
40. Li, T., Xu, W., Ouyang, J., Lu, X., Sherchan, P., Lenahan, C., Irio, G., Zhang, J.H., Zhao, J., Zhang, Y., and Tang, J. (2020). Orexin A alleviates neuroinflammation via OXR2/CaMKKβ/AMPK signaling pathway after ICH in mice. J. Neuroinflammation *17*, 187.
41. Wang, Y., Tian, M., Tan, J., Pei, X., Lu, C., Xin, Y., Deng, S., Zhao, F., Gao, Y., and Gong, Y. (2022). Irisin ameliorates neuroinflammation and neuronal apoptosis through integrin αVβ5/AMPK signaling pathway after intracerebral hemorrhage in mice. J. Neuroinflammation *19*, 82.

STAR★METHODS

KEY RESOURCES TABLE

REAGENT or RESOURCE	SOURCE	IDENTIFIER
Antibodies		
SENP1 Rabbit polyclonal antibody	Affinity	AF0275; RRID: AB_2833445
NeuN Rabbit monoclonal antibody	Abcam	ab177487; RRID: AB_2532109
GFAP Rabbit polyclonal antibody	Abcam	ab7260; RRID: AB_305808
LC3 Rabbit monoclonal antibody	Abcam	ab192890; RRID: AB_2827794
p62 Rabbit monoclonal antibody	Abcam	ab109012; RRID: AB_2810880
OPTN Rabbit monoclonal antibody	Abcam	ab213556; RRID: AB_2890221
SUMO1 Rabbit monoclonal antibody	Abcam	ab32058; RRID: AB_778173
COX IV Rabbit monoclonal antibody	Abcam	ab202554; RRID: AB_2861351
GAPDH Mouse monoclonal antibody	Abcam	ab181602; RRID: AB_2630358
Goat anti-Rabbit IgG (H + L) Secondary Antibody, HRP	Invitrogen	31460; RRID: AB_228341
Goat Anti-Mouse IgG H&L (HRP)	Abcam	ab6789; RRID: AB_955439
Bacterial and virus strains		
sh-SENP1	GenePharma	N/A
sh-OPTN	GenePharma	N/A
oe-SENP1	OBiO Technology	N/A
oe-OPTN	OBiO Technology	N/A
Chemicals, peptides, and recombinant proteins		
FBS	Gibco	A5669701
DMEM/F12	Gibco	11320033
PBS	Gibco	14190144
DAPI	Beyotime	C1002
ECL detection system	Thermo Fisher Scientific	34096
TRIzol	Invitrogen	15596026
Triton X-100	Beyotime	P0096
PVDF membrane	Beyotime	FFP39
EdU	Thermo Fisher Scientific	A10044
IP lysis buffer	Beyotime	P0013
Critical commercial assays		
In situ Cell Death Detection kit	Roche	12156792910
FJC ready-to-dilute staining kit	Biosensis	TR-100-FJT
Cell Mitochondria Isolation Kit	Beyotime	C3601
BCA Protein Quantification Kit	Thermo Fisher Scientific	23225
One Step TB Green® PrimeScript™ RT-PCR Kit	Takara	RR086A
Experimental models: Organisms/strains		
Sprague-Dawley rats	Shandong Laboratory Animal Center	N/A
Oligonucleotides		
SENP1 Forward: 5′-CGTTCTTCCAGGCAGAGCTATG-3′	This paper	N/A
SENP1 Reverse: 5′- GCTGTAGTGCCAATGCTTTCTGC-3′	This paper	N/A
GAPDH Forward: 5′- CATCACTGCCACCCAGAAGACTG-3′	This paper	N/A
GAPDH Reverse: 5′- ATGCCAGTGAGCTTCCCGTTCAG-3′	This paper	N/A

(*Continued on next page*)

Continued

REAGENT or RESOURCE	SOURCE	IDENTIFIER
Software and algorithms		
SPSS software	SPSS Inc.	Version 26.0
Prism	GraphPad Software	Version 8.0.0

RESOURCE AVAILABILITY

Lead contact

Further information and requests for resources and reagents should be directed to and will be fulfilled by the Lead Contact, Ying Xia (xiaying0509@163.com).

Materials availability

This study did not generate new unique reagents.

Data and code availability

Western blot original data have been deposited at Mendeley and publicly available as of the date of publication. The DOI and accession numbers are listed in the key resources table. This paper does not report any original code. Any additional information required to reanalyze the data reported in this paper is available from the lead contact upon request.

EXPERIMENTAL MODEL AND STUDY PARTICIPANT DETAILS

Animals

Male Sprague Dawley (SD) rats (280–300 g) were purchased from Shandong Laboratory Animal Center (Jinan, Shandong, China). All animal experiments were approved by the Animal Care Committee of the Haikou Affiliated Hospital of Central South University Xiangya School of Medicine and all procedures were performed in accordance with relevant regulations.

METHOD DETAILS

Cell culture

OM-MSCs got from olfactory mucosa in SD rats (Shandong Laboratory Animal Center, Jinan, Shandong, China).[35] Snipped nasal mucosa tissues were cultured in DMEM/F12 medium containing 15% FBS (Gibco, Grand Island, NY, USA) for 3 days. The OM-MSCs were extended to 80% integration. The purified OM-MSCs were detected by immunofluorescence method. Moreover, cells were regularly tested for mycoplasma contamination.

Cell transfection

To knockdown SENP1 or OPTN expression, short hairpin RNAs (shRNAs) targeting SENP1 or OPTN (sh-SENP1 or sh-OPTN) and negative control shRNA (sh-NC) were synthesized and expressed in the adenovirus (Ad) vectors (GenePharma, Shanghai, China). For overexpression of SENP1 or OPTN, pcDNA3.1-SENP1 or OPTN vector (termed oe-SENP1 or oe-OPTN) and an empty pcDNA3.1 vector (termed oe-NC) expressed in the Ad vectors were purchased from OBiO Technology (Shanghai, China). The cultured OM-MSCs were infected with the respective Ad at an optimal multiplicity of infection of 100.

Differentiation of OM-MSCs

To induce neuronal differentiation, OM-MSCs were cultured in DMEM/F12 medium containing retinoic acid (1 μM; Sigma-Aldrich, St. Louis, MO, USA) and forskolin (5 μM; Sigma-Aldrich) for 4 days. To induce astrocytic differentiation, OM-MSCs were incubated with medium containing leukemia inhibitory factor (50 ng/mL; Yeasen, Shanghai, China) and Bone morphogenetic protein 2 (50 ng/mL; MedChem Express, Monmouth Junction, NJ, USA) for 6 days. After differentiation induction, the cells were tested for specific genes, including neuron specific gene (NeuN) and astrocyte specific gene (GFAP).[36,37]

ICH model establishment

The rats were placed at a constant ambient temperature (23 ± 2°C), light and dark cycle for 12 h, and freely fed and drank. The ICH model was induced using the autologous blood injection method.[38] Rats were anesthetized in the anesthesia room at 5 L/min oxygen flow and 8% isoflurane, and under a mask at 2 L/min oxygen flow and 4% isoflurane. Then, the rats were fixed in the stereotactic apparatus, and 50 μL of caudal artery blood was injected into the caudate nucleus of the right basal ganglia with an injection pump at a rate of 5 μL/min. The coordinates are 0.2 mm anterior pleura, 3.5 mm lateral pleura, and 6.0 mm depth. The rats in sham group were injected with the same amount of normal saline.

All animal experiments were approved by the Animal Care Committee of the Haikou Affiliated Hospital of Central South University Xiangya School of Medicine.

OM-MSCs intracerebral transplantation

The animals were randomized into the following groups (n = 6 per group): sham, ICH, ICH + OM-MSCs, ICH + OM-MSCs oe-NC (OM-MSCs transfected with oe-NC were injected into ICH rats), ICH + OM-MSCs oe-SENP1 (OM-MSCs transfected with oe-SENP1 were injected into ICH rats), and ICH + OM-MSCs oe-OPTN (OM-MSCs transfected with oe-OPTN were injected into ICH rats). For OM-MSCs treated groups, OM-MSCs (2×10^6) in 2 μL saline were stereotactically injected into the edge of ipsilateral lesion with a rate of 0.1 μL/min at 6 h after ICH modeling. For the ICH group, 2 μL saline was administrated to the same position.

Determination of cerebral water content

The brains of the killed rats were removed immediately and cut into five parts: ipsilateral cortex, ipsilateral basal ganglion, contralateral basal ganglion, cerebellum, and contralateral cortex. Each brain slice was detected on an analytical microbalance to obtain wet weight (WW). Then, the brain parts were roasted at 100°C for 48 h to obtain dry weight (DW). The measurement formula of brain water content (%) is (WW − DW)/WW × 100%.[39]

Neurobehavioral tests

Modifed Garcia score test, forelimb placement test, and corner turn test were performed to assess short-term neurofunctional behavior of ICH rats. The modified Garcia test consisted of seven separate tests: axial sensation, spontaneous movement, limb symmetry, tactile proprioception, forelimb extension, side turn, and climbing. Each trial was scored on a scale of 0–3, with 0 being the worst and 3 the best. Neurological function was evaluated by adding the scores of the seven trials on a scale of 0–21.[40] The forelimb placement test was performed by holding the rat's torso and stroking its left tentacles along the edge of the platform. The results were interpreted as the number of times the left forelimb was placed on the platform as a percentage of the total number of tentacle strokes. A total of 10 times of rats were recorded in the corner turn test (a 30° angle corner). The score was calculated according to the number of left turns/10 times × 100%.

Immunofluorescence

OM-MSCs laid on orifice plates were fixed with 4% paraformaldehyde and incubated with primary antibody. The following antibodies are used for staining: NeuN (1/300; ab177487, Abcam, Cambridge, MA, USA) and GFAP (1/5000; ab7260, Abcam). Then, cells were incubated with corresponding secondary antibodies, and nuclei were stained with DAPI (Beyotime, Shanghai, China). A fluorescence microscope (Leica, Wetzlar, Germany) was used to acquire images for analysis. Frozen sections (4 μm thick) were obtained from the cerebral hemorrhage area of each animal, infiltrated with 0.5% Triton X-100, and incubated overnight with NueN (1:100) antibody at 4°C. Alexa Fluor488-conjugated goat rabbit IgG was used to localize signals. Finally, DAPI was used to reverse stain the sections and images were observed under a fluorescence microscope (Leica).

TUNEL staining

In situ Cell Death Detection kit (Roche, USA) was utilized to assess neuronal cell apoptosis at 72 h after ICH via the staining of TUNEL. The number of TUNEL-positive cells in 6 sections of each brain was manually counted by using the ImageJ software (ImageJ, Version 1.4, NIH, Bethesda, MD, USA). The data were expressed as the percentage of TUNEL positive neurons (%).

Fluoro-Jade C (FJC) staining

Degenerative neurons were stained with a modified FJC ready-to-dilute staining kit (Biosensis, USA). The slides were washed in PBS, incubated with FJC working solution for 20 min, and then observed under a fluorescence microscope (Leica). FJC-positive neurons were manually counted in the perihematoma area at six sites in each brain using the ImageJ software. The data were averaged and presented as positive cells/mm^2.[41]

5-Ethynyl-2′-deoxyuridine (EdU) staining

OM-MSCs were placed in glass substrate with a density of 1×10^5 cells and treated with a EdU working solution (Thermo Fisher Scientific, Waltham, MA, USA). The cell culture medium of each group was replaced with the mixture and incubated for 2 h at 37°C. After incubation, the cells were fixed with 4% paraformaldehyde for 30 min. Cells were permeated on ice with 0.1% Triton X-100 for 2 min and washed with PBS. The nuclei were stained with DAPI (Beyotime). Images were obtained using confocal fluorescence microscopy and the percentage of EdU positive cells was calculated.

Western blot

Total protein from cells or brain tissues was isolated by RIPA buffer (Beyotime). In addition, mitochondria were isolated from the cytoplasm using the Cell Mitochondria Isolation Kit (Beyotime) and incubated with the mitochondrial lysis buffer supplemented with PMSF (Beyotime) to

extract mitochondrial proteins. After quantification using BCA Protein Quantification Kit (Thermo Fisher Scientific), equal amounts of proteins were loaded onto an SDS-PAGE gel for separation. Subsequently, the protein signal was transferred onto the PVDF membrane and blocked by 5% non-fat milk powder. The membrane was incubated with primary antibodies against SENP1 (1/1000; AF0275, Affinity), NeuN (1/2000; ab177487, Abcam), GFAP (1/10000; ab7260, Abcam), LC3 (1/2000; ab192890, Abcam), p62 (1/10000, ab109012, Abcam), OPTN (1/1000; ab213556, Abcam), COX IV (1/2000; ab202554, Abcam) and GAPDH (1/10000; ab181602, Abcam) overnight at 4°C. After incubating with appropriate secondary antibody at 37°C for 1 h, the blot was visualized using ECL detection system (Thermo Fisher Scientific). Relative protein levels were assessed by ImageJ software.

Immunoprecipitation (IP)

To measure the SUMOylation of OPTN in endogenous level, transfected OM-MSCs were washed three times with cold PBS and then cleaved in IP lysis buffer. Cell lysates were centrifuged (12000 *g*, 4°C) and supernatants were precipitated by OPTN antibody (1/40; ab213556, Abcam) and IgG (negative control). Protein A/G agarose beads were added to the cells and incubated overnight at 4°C. The washed precipitated proteins were detected by Western blotting with SUMO1 (1/1000; ab32058, Abcam), SENP1 and OPTN.

qPCR assay

Total RNA extraction was performed using TRIzol reagent (Invitrogen, USA), and reverse transcribed into cDNA using One Step TB Green PrimeScript RT-PCR Kit (Takara, Japan) and then quantified with specific primers on Applied Biosystems 7300 Real-Time PCR System (Thermo Fisher Scientific). GAPDH mRNA was employed as control, and $2^{-\Delta\Delta Ct}$ formula was used to calculate relative gene levels. The primers used in this study were listed as follows: SENP1 (Forward: 5′-CGT TCT TCC AGG CAG AGC TAT G-3′, Reverse: 5′-GCT GTA GTG CCA ATG CTT TCT GC-3′) and GAPDH (Forward: 5′-CAT CAC TGC CAC CCA GAA GAC TG-3′, Reverse: 5′-ATG CCA GTG AGC TTC CCG TTC AG-3′).

Mitophagy evaluation

OM-MSCs were briefly transfected with GFP-mRFP-LC3 adenovirus (20 multiplicity of infection; Hanbio, Shanghai, China) for 24 h, and Mito-Tracker Deep Red (30 min at 37°C; Beyotime) was used to detect the localization of mitochondria. The nuclei were stained with DAPI (Beyotime). Yellow dots were detected in at least 100 cells in each individual experiment by confocal microscopy after different treatments. Image Pro-Plus software was used to assess the degree of co-location using Manders overlap coefficients.

QUANTIFICATION AND STATISTICAL ANALYSIS

Statistics are presented as the mean ± standard deviation (SD) and analyzed using SPSS 26.0 (SPSS Inc., Chicago, IL, USA) and GraphPad Prism 8.0 (Graph-Pad Software, USA). The difference between two groups was determined using Student's t test. Statistical difference among multiple groups was determined using one-way analysis of variance (ANOVA) test followed by Tukey multiple-comparison post hoc analysis. $p < 0.05$ was considered statistically significant. Statistical significance was set at as $^{*}p < 0.05$, $^{**}p < 0.01$, and $^{***}p < 0.001$.